water

MDPI

Article

Application of a Single Porous Basket as a Pier Scour Countermeasure

Wei-Lin Lee [1], Chih-Wei Lu [2,*] and Chin-Kun Huang [1]

[1] Department of Hydraulics and Ocean Engineering, National Cheng Kung University, Tainan 701401, Taiwan; glaciallife@gmail.com (W.-L.L.); ckhuang@mail.ncku.edu.tw (C.-K.H.)
[2] Department of Civil and Construction Engineering, National Taiwan University of Science and Technology, Taipei 106335, Taiwan
* Correspondence: cwlu@mail.ntust.edu.tw; Tel.: +886-2-2737-6563

Abstract: This paper presents a study on bridge pier protection with a single porous basket (SPB) in clear-water experiments. The SPB is a type of combined flow-altering countermeasure. The SPB was installed at a distance ahead of the protected pier. After a series of tests, the results showed that appropriate installation of the SPB was able to effectively adjust the flow pattern to reduce the down-flow motion and horseshoe vortex ahead of the pier. Dominant factors for the pier protection—considered for all tests—included the distance between the basket and pier, submerged depth of the basket, basket length, pier diameter, basket diameter, hole size, porosity, and the flow approaching angle. After evaluating these parameters through laboratory tests, the results of protection were optimized. In optimal conditions, the SPB was able to provide maximum pier protection and decrease the maximum scour depth by as much as 75.53%.

Keywords: porous cylinder; scour protection; bridge pier

check for updates

Citation: Lee, W.-L.; Lu, C.-W.; Huang, C.-K. Application of a Single Porous Basket as a Pier Scour Countermeasure. *Water* **2021**, *13*, 3052. https://doi.org/10.3390/w13213052

Academic Editors: Michele Palermo and Stefano Pagliara

Received: 31 August 2021
Accepted: 30 October 2021
Published: 1 November 2021

Publisher's Note: MDPI stays neutral with regard to jurisdictional claims in published maps and institutional affiliations.

Copyright: © 2021 by the authors. Licensee MDPI, Basel, Switzerland. This article is an open access article distributed under the terms and conditions of the Creative Commons Attribution (CC BY) license (https://creativecommons.org/licenses/by/4.0/).

1. Introduction

Protection of bridge piers against local scour is a major concern of bridge maintenance. The safety of bridges is seriously threatened by river floods during typhoons or thunderstorms. In Taiwan, floods caused by typhoons are often so violent as to displace a large amount of bed sediment and drift in rivers. The average flow velocity of a flooded river is typically between 3 m/s and 8 m/s, several times faster than that of the regular flow speed. The peak discharge of a flood is quite sharp and concentrated due to the short and steep slope of the riverbed in the narrow territory of Taiwan island [1]. Tremendous protection work on bridge piers has been carried out in Taiwan; one of the typical protection methods is to adopt an armor unit made of concrete for wave energy dissipating such as in Figure 1a [2]. In Figure 1a, it can clearly be seen that the contractor made a highly conservative design to armor the whole region of bridge piers by using many concrete blocks. However, after a flood, the concrete blocks between the piers were swept away in Figure 1b. It also implied that the riverbed that the swept blocks rested on was scoured, which symbolizes that it is inappropriate to locate concrete blocks as protection work in these kinds of conditions due to the additional contraction which would be caused by the concrete blocks. Another practical problem in Taiwan, the bridge could be toppled by the flow due to a large amount of drift. For example, on 8 August 2009, a total of 20 bridges, including the Dajin and Liukuei bridges on Provincial Highway 27, Shuangyuan Bridge on Highway 17, Sinciwei and Mingtzu bridges on Highway 21, No. 1 Bridge on Highway 24, and Ciwei Bridge on Highway 28, were either damaged or washed away due to Typhoon Morakot. As shown in Figure 1c, a bridge stood in the course of flood flow caused by the heavy rain and collapsed after toppling and some piers falling. Figure 1d showed that an example of bridge piers blocked by the drifts. The above-mentioned examples provide

evidence that seeking more effective ways to protect bridge piers from scouring is urgent and practically important.



Figure 1. Images of bridge piers. (**a**) Protected by several concrete blocks; (**b**) concrete blocks were washed away after a flood at the same site as (**a**); (**c**) failure of Ciwei Bridge, Cishan River, Taiwan, in August 2009; (**d**) drifts stuck between bridge piers; (**e**) protective effect of SPB from drifts.

To relieve local scour near bridge piers, Melville and Hadfield (1999) indicated that the bed resistance against scour is not only strengthened by using armor devices, but also allows for adjusting the flow patterns around the pier by flow-altering devices [3]. A well-designed flow-altering device can deflect the flow to minimize scouring, as well as induce deposition in the local scour hole near the pier. Several methods frequently used to change the surrounding flow pattern are: (1) placing a collar plate near the base of piers to mitigate the down-flow motion [4,5]; (2) setting up sacrificial piles in the front of the pier to weaken the pier scouring [3,5]; (3) installing the counter-eddy bottom panels

(such as Iowa vans) to decrease the eddy near the pier [5,6]; (4) using surface guide panels to decrease the flow velocity around the pier [5,7,8]; and (5) allowing a portion of the approach flow to pass through the openings inside a pier or among smaller piers to reduce the strength of the downflow and the horseshoe vortex [5]. Another option is combined flow-altering countermeasures against bridge pier scour [9]. A new combined flow-altering countermeasure, known as "single porous basket (SPB)", is proposed in this study. An SPB is similar to a sacrificial pile in front of the pier, the capability of the porous basket is similar to the surface guide panel, and it allows the approach flow to pass through. Figure 1e presents the performances of two sets of SPB groups used in the field in contrast to Figure 1d. This SPB group is able to rotate during the flood; therefore, the drifts are spun off from the SPB and are able to pass through the piers more easily. The cost and the maintenance of the SPB are cheaper and easier than the bed-armoring countermeasures, offering an advantage in practical work. Hence, this paper is interested in investigating the performance of the SPB on the reduction in local scour near bridge piers.

In this paper, the capability of an SBP is introduced and a series of experiments were conducted to evaluate all the influential parameters in order to uncover the optimum protection that the SPB can provide for scouring the river bed. The effects of flow features, sediment features, and bridge pier geometry on pier scour have been investigated in a series of laboratory works. Some researchers have focused on the flow feature, for example, Melville and Coleman (2000) illustrated the relationship of flow intensity and local scour depth by their experimental results and highlighted the critical conditions for the occurrence of local scour [10]. Ettema et al. (1998) and Bozkus and Yildiz (2004) implemented a series of laboratory works and derived empirical formulas to estimate the local scour depth using Froude number of approach flow, flow depth, and pier diameter [11,12]. Furthermore, some researchers have focused on the sediment feature, for example, Ettema (1980) found that the local scour depth changed with median distribution size (d_{50}) and its relationship with sediment coarseness was introduced [13]. Chiew (1984) and Baker (1986) implemented experiments in live-bed conditions with non-uniform bed material and discussed the effect of sediment non-uniformity on the local scour depth [14,15]. Moreover, researchers have focused on the bridge pier geometry; for example, Chee (1982) and Raudkivi (1986) implemented experiments with different flow depth and pier diameter conditions [16,17], and Melville (2008) discussed the relationship of local depth and pier diameter using flow shallowness [18]. According to the aforementioned research, the importance of flow features, sediment features, and bridge pier geometry has been highlighted. The experimental research on SPBs has rarely been discussed in previous studies, and this study discusses the protective effect of SPBs, focusing on the geometric feature between the SPB and the bridge pier. The other protective effects of the SPB, such as use as a group and protection from drifts, are beyond the scope of this research.

In the present study, the protective effect of a single porous basket (SPB)—a new type of combined flow-altering countermeasure—is investigated by a series of experiments. In Section 2, the major factors of the protective effect of SPBs are introduced. Section 3 introduces the study's experimental procedures. Section 4 discusses and illustrates the protective effect of SPBs related to the geometric features, including the influence of SPB porosity, hole size, height, distance between basket and bridge pier, and attack angle of approach flow. Section 5 concludes with the most optimal SPB conditions and its protective effects.

2. Similitude of Approach Flow around Single Porous Basket

Figure 2 shows the mechanism of water flowing through the SPB. The SPB was set on the bed surface in front of the bridge pier and fixed by piles—it only has the porous basket on the upper part; the diameter of the lower part is smaller than that of the basket. The flow, therefore, can pass through the bottom of the SPB. The single porous basket placed upstream of the protected pier primarily influences the scour around the protected pier in two ways. First, when the flow passes through the SPB, the velocity will drop in the

shadow area owing to the porous effect. Hence, the down-flow ahead of the protected pier and the horseshoe-vortex around the pier body will be weakened, and the depth of scouring nearby the protected pier will be smaller. In this manner, the SPB produces a sheltering effect for the protected pier. Secondly, the formation of the deposition ridge behind the SPB, as schematically shown in Figure 2, affects the scour hole development at the protected pier. It is clear that the deposition ridge alters the flow field in front of the pier by causing the flow to be diverted to the sides of the deposition ridge and, thereby, reducing the erosive power of the flow over the deposition ridge. As a result, a reduction in scour depth at the pier is observed. In this article, we show the effectiveness of reducing the pier scour depth utilizing the SPB, which not only acquires favorably reduced velocity but also drives more sands from upstream and retains them in the scour hole of the pier.

The major parameters in SPB setup for pier scour protection in clear water, as shown in Figure 3, can be categorized by the following factors:

1. Flow condition factors: water depth H, flow velocity V, fluid density ρ, kinematic viscosity of water ν, and gravity acceleration g;
2. Bed sediment factors: particle shape factor K_d, standard deviation in geometric size distribution σ_g, sand density ρ_s, and median distribution size d_{50};
3. Pier geometry factors: pier shape factor K_p, pier diameter b, and flow approaching angle to the pier axis α;
4. SPB setup factors: basket diameter D, basket shape factor K_l, basket length B_l, distance from the protected pier L, hole size d, attack angle of approach flow θ, and porosity e.

The attack angle θ is the angle between the direction of flow and the center line from the pier to the basket, the partial flow directly attacks the pier, as shown in the plan view of Figure 3.

The porosity e is the proportion of porous holes,

$$e = \frac{A}{A_0}, \tag{1}$$

where A and A_0 are, respectively, the net hole area and the total surface area of the basket. Therefore, at $e = 0$ the flow cannot penetrate the basket, and at $e = 1$, the porous basket is absent.

The maximum scour depth of the pier, d_s, can, therefore, be a function of:

$$d_s = f_1\left(H, V, \rho, \nu, g, K_d, \sigma_g, \rho_s, d_{50}, K_p, b, \alpha, D, K_l, B_l, L, d, \theta, e\right). \tag{2}$$

According to law of similitude, Equation (2) is rewritten:

$$\frac{d_s}{b} = f_1\left(\frac{H}{b}, \frac{V}{\sqrt{gh}}, \frac{\rho}{\rho_s}, \frac{Vd_{50}}{\nu}, K_d, \sigma_g, K_p, \alpha, \frac{D}{b}, K_l, \frac{B_l}{H}, \frac{L}{b}, \frac{d}{D}, \theta, e\right). \tag{3}$$

For laboratory experiments, the parameters H, V, ρ, ν, g, K_d, σ_g, ρ_s, d_{50}, K_p, b, α, and K_l are fixed. Under this condition, Equation (3) can be simplified to:

$$\frac{d_s}{b} = f_1\left(\frac{D}{b}, \frac{B_l}{H}, \frac{L}{b}, \frac{d}{D}, e, \theta\right). \tag{4}$$

In the present study, we discuss the influence of these six parameters in Equation (4) on the pier scour according to the laboratory test results. The kinematic similarity and dynamic similarity were not investigated in this study, therefore, the protective effect of SPBs against different flow conditions was not discussed.

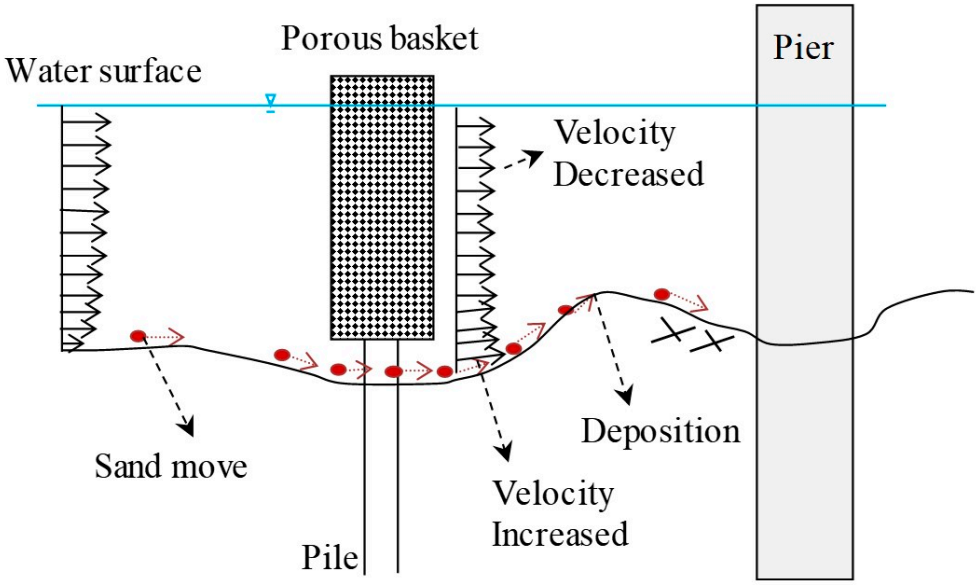


Figure 2. The pattern of the flow passing through the single porous basket.

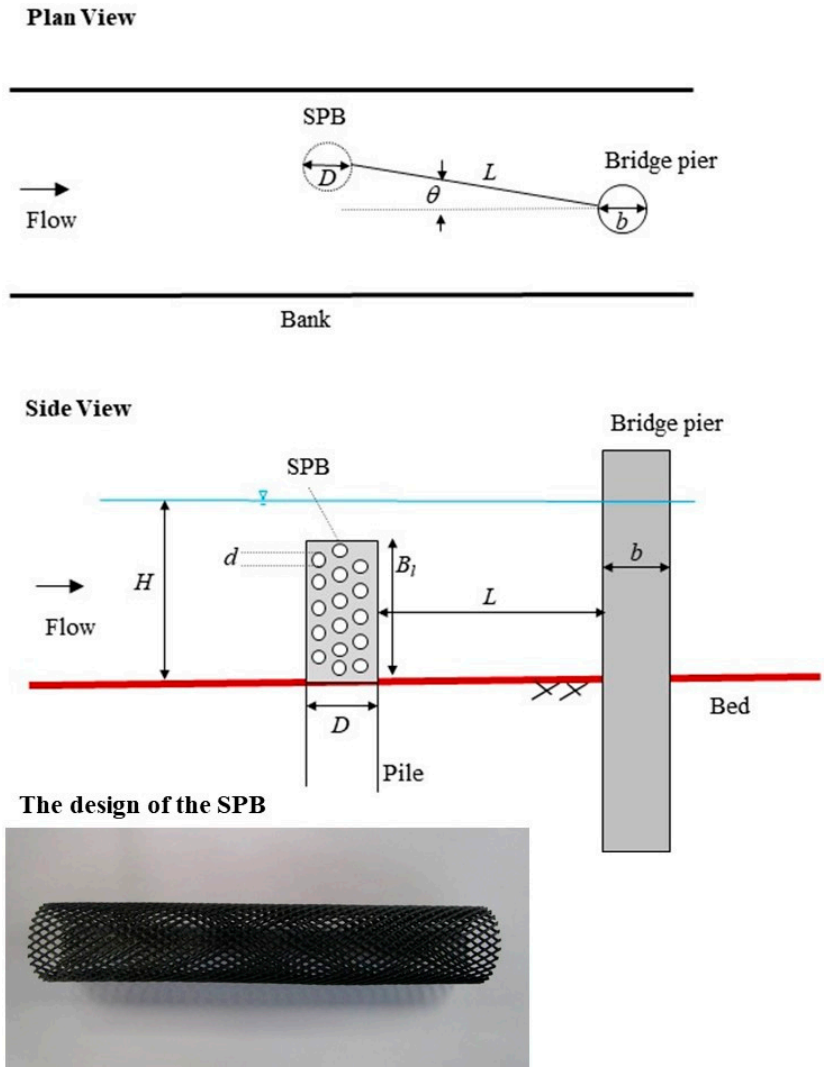


Figure 3. Scheme of experimental set-up of the pier and the SPB.

3. Procedure of the Experimental Work

3.1. Experimental Set-Up

We conducted the clear-water experiment in a 60 cm wide (B), 38 cm deep, and 1040 cm long flume, as shown in Figure 4. The live bed in the experiment was filled with sand, of which the density was ρ_s = 2600 kg/m^3, the median of the size distribution was d_{50} = 0.515 mm, and the standard deviation of the size distribution was σ_g = 1.064. The effect of the armor can be avoided as $\sigma_g < 1.3$ [19]. The cylindrical bridge pier model was made of polystyrene pipe of diameter b = 8 cm. When b/d_{50} is larger than 50, the local depth is not influenced by sediment size [10]. A flow rate of 0.0077 m^3/s was used, and the water depth H was 6 cm. In the flume, the average velocity (V) was 0.2146 m/s, and the Froude number was 0.28. The flow intensity (V/V_c) can be estimated as follows:

$$\frac{V}{V_c} = 5.75 \times \log\left[5.53 \times \left(\frac{H}{d_{50}}\right)\right]. \quad (5)$$

where V_c is the critical velocity for sediment startup movement [10]. The critical velocity (V_c) for the sediment used in this study can be determined using the Shields diagram as 0.019 m/s [20]. Therefore, in this study, the flow intensity was maintained as 0.7, and satisfies the occurrence condition of scour in clear water ($V/V_c > 0.5$) [10]. The aforementioned conditions in this study are the control variables, and the flow and pier setup conditions are summarized in Table 1.

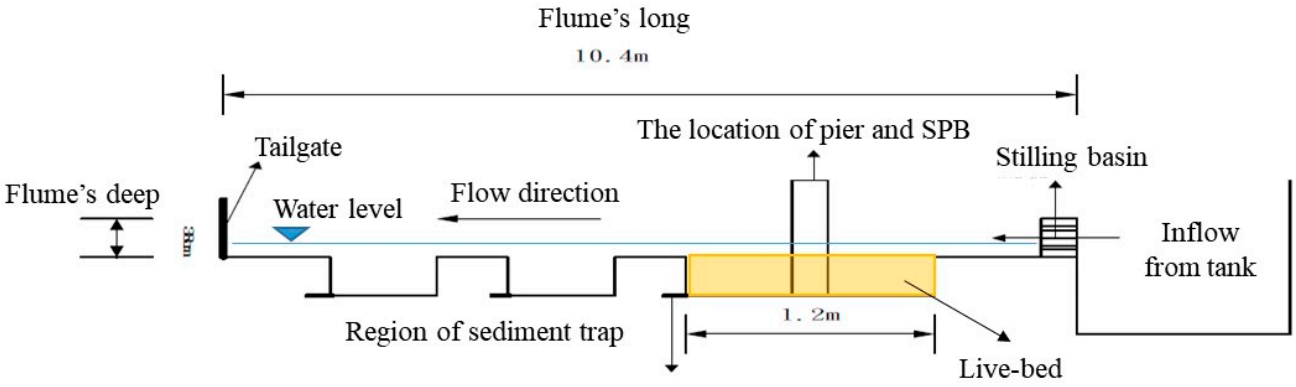


Figure 4. Schematic diagram of the experimental flume.

Table 1. Experimental conditions.

V (m/s)	H (cm)	d_{50} (mm)	σ	b (cm)	F_r	V/V_c	ρ_s/ρ	H/b
0.2146	6	0.515	1.064	8	0.280	0.7	2.6	0.75

3.2. Experimental Procedure

The experimental procedure can be divided into two parts. First, the installation of SPBs is given according to the experimental designs. Second, the spatial distribution of local scour depth is measured after reaching an equilibrium state. These procedures were introduced as follows.

A set of the SPBs was installed vertically into the laboratory flume with a basket length B_l, at a distance L ahead of the pier, as shown in Figure 3. The geometric conditions of the SPB, which included basket diameter (D), basket length (B_l), distance from the protected pier (L), hole size (d), attack angle of approach flow (θ), and porosity (e), were independent variables in this study. In the following tests, the protective effect against bridge pier scour with the SPB—considering six parameters—was investigated. In order to investigate the effect of protection against different geometric conditions, the running cases were divided into five sets, as shown in Table 2. In the experiment of group A, nine experiments were

conducted by testing three different hole sizes (i.e., d = 3, 4, and 5 mm) and three different porosities (i.e., e = 0.2, 0.4, and 0.5). In the experiment of group B, nine experiments were performed by testing nine different distances from the protected pier (i.e., L = 0, 40, 80, 120, 160, 200, 240, 280, and 560 mm) In the experiment of group C, five experiments were implemented by testing five different basket lengths (i.e., B_l = 0, 20, 30, 60, and 80 mm). In the experiment of group D, four experiments were conducted by testing four different basket diameters (i.e., D = 14, 21, 34, and 80 mm). In the experiment of group E, three experiments were performed by testing three different approach flow attack angles (i.e., θ = 0, 30, and 45 degree). In the case of PP, the experiment was performed without any structure in front of the protected pier. Last, in the case of OR (e = 0), there was a pier which had no hole for the approach flow to pass through, which was installed ahead of the protected pier.

Table 2. Studied cases and protective effect.

Case	d mm	e	D mm	L mm	B_l mm	θ degree	d_s mm	d_s/b	P %
PP		Without protection					103.0	1.29	18.93
OR	0	0	80	80	80	0	83.5	1.04	18.93
A1	3	0.2	80	80	80	0	55.5	0.69	46.12
A2	3	0.4	80	80	80	0	44.7	0.56	56.60
A3	3	0.5	80	80	80	0	41.5	0.52	59.71
A4	4	0.2	80	80	80	0	60.0	0.75	41.75
A5	4	0.4	80	80	80	0	44.2	0.55	57.09
A6 *	4	0.5	80	80	80	0	25.2	0.32	75.53
A7	5	0.2	80	80	80	0	64.3	0.80	37.57
A8	5	0.4	80	80	80	0	53.0	0.66	48.54
A9	5	0.5	80	80	80	0	30.7	0.38	70.19
B1	4	0.5	80	0	80	0	52.5	0.66	49.03
B2	4	0.5	80	40	80	0	37.5	0.47	63.59
B3 *	4	0.5	80	80	80	0	25.2	0.32	75.53
B4	4	0.5	80	120	80	0	41.5	0.52	59.71
B5	4	0.5	80	160	80	0	40.2	0.50	60.97
B6	4	0.5	80	200	80	0	50.4	0.63	51.07
B7	4	0.5	80	240	80	0	51.0	0.64	50.49
B8	4	0.5	80	280	80	0	59.5	0.74	42.23
B9	4	0.5	80	560	80	0	64.8	0.81	37.09
C1	4	0.5	80	80	0	0	103.0	1.29	0.00
C2	4	0.5	80	80	20	0	72.7	0.91	29.42
C3	4	0.5	80	80	30	0	66.5	0.83	35.44
C4	4	0.5	80	80	60	0	60.5	0.76	41.26
C5 *	4	0.5	80	80	80	0	25.2	0.32	75.53
D1	3	0.5	14	80	80	0	79.0	0.99	23.30
D2	3	0.5	21	80	80	0	61.2	0.77	40.58
D3	3	0.5	34	80	80	0	53.8	0.67	47.77
D4 *	4	0.5	80	80	80	0	25.2	0.32	75.53
E1 *	4	0.5	80	80	80	0	25.2	0.32	75.53
E2	4	0.5	80	80	80	30	89.8	1.12	12.82
E3	4	0.5	80	80	80	45	114.5	1.43	−11.17

* Cases with the same condition.

To obtain the equilibrium scour depth in clear-water conditions, a 24 h preliminary test was performed. Figure 5 demonstrates the scour depth of an unprotected and protected pier as time flows. As the local scour in clear-water conditions can take a very long time to reach an equilibrium state [21], it is crucial to determine a suitable running time for each test in order to conserve time while the test results can still represent the protection

provided by the tested SPB. A criterion can be derived for the equilibrium condition: a variation of $d_s < 0.05b$ in 24 h [21]. As shown in Figure 5, in the 24 h test with the SPB, the depth of local scour is kept at a fixed value in the 4 h run time; in the test without the SPB, at the fourth hour, local scour depth had reached more than 83% of that at the 24th hour. Accordingly, the protective effect of the SPB can be estimated at the fourth hour, and the protective effect of the SPB increased depending on time. Therefore, the running time for each test, set at four hours in this paper, is enough to show the protective effect of the SPB.

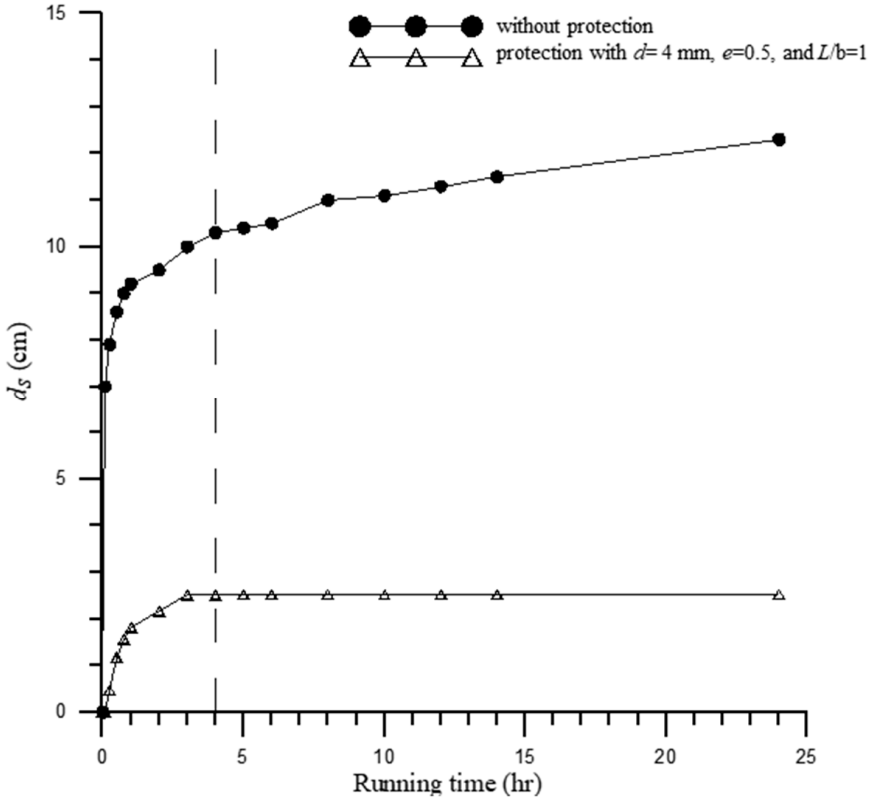


Figure 5. Duration of the scouring depth of the bridge pier with or without the SPB.

The topography was measured after the local scour reached equilibrium, and the protective effect can be discussed based on the experimental results. The topography of pier scour without the SPB is shown in Figure 6. The area affected by scouring was around the pier and the maximum value of scour depth was located in front of the pier. In the case with the SPB protecting the pier in the conditions d = 4.5 mm, e = 0.5, and L/b = 1, as shown in Figure 7, the area representing higher scour was located around the basket. The region behind the basket demonstrated less scour because the basket had weakened the flow force. The highest scour around the pier took place at its sides, not in front of the pier. The scour depth of the basket itself was smaller than that of the pier scouring because the basket was a porous structure. Then, the effect of bridge pier protection with the SPB can be defined by the reduction percentage of scour depth, P:

$$P = \left(\frac{d_{sn} - d_s}{d_{sn}} \right) \times 100\% \quad (6)$$

where d_{sn} is the maximum scour depth of the pier without the SPB and d_s is the maximum scour depth of the pier with the SPB protection. Accordingly, d_{sn} was 103 mm, and d_s was 25.2 mm in the case of d = 4 mm, e = 0.5, and L/b = 1. With the help of Equation (6), the protection can be read as 75.53%.

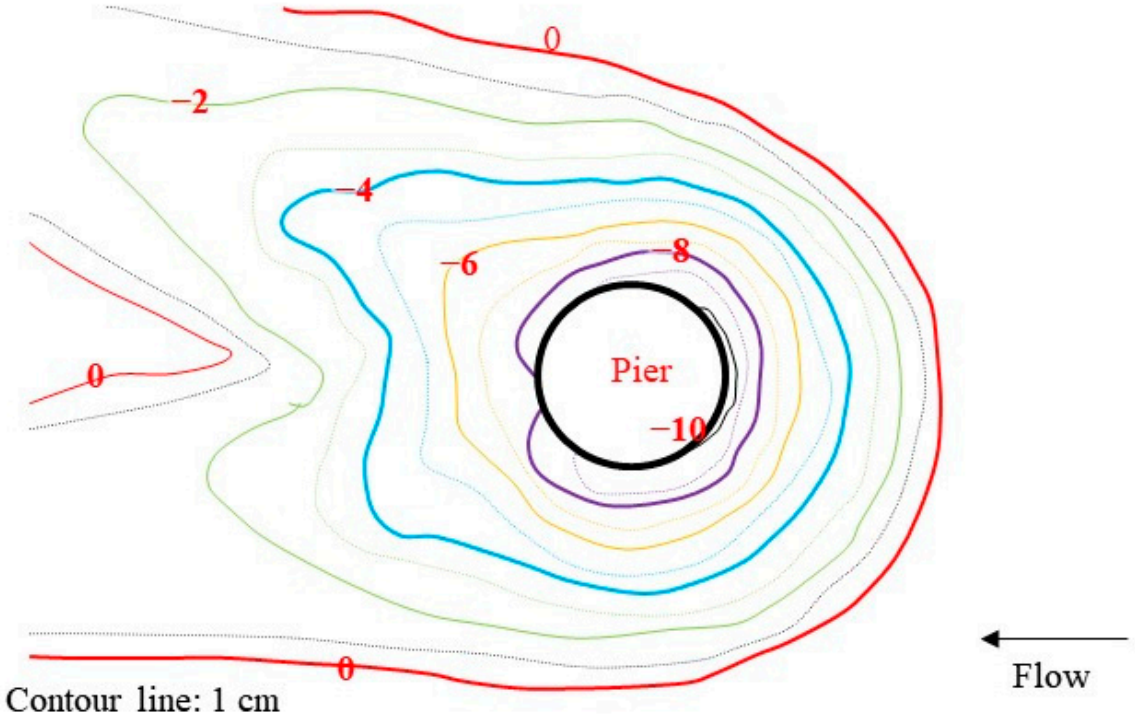


Figure 6. Topography of pure pier scours without the SPB.

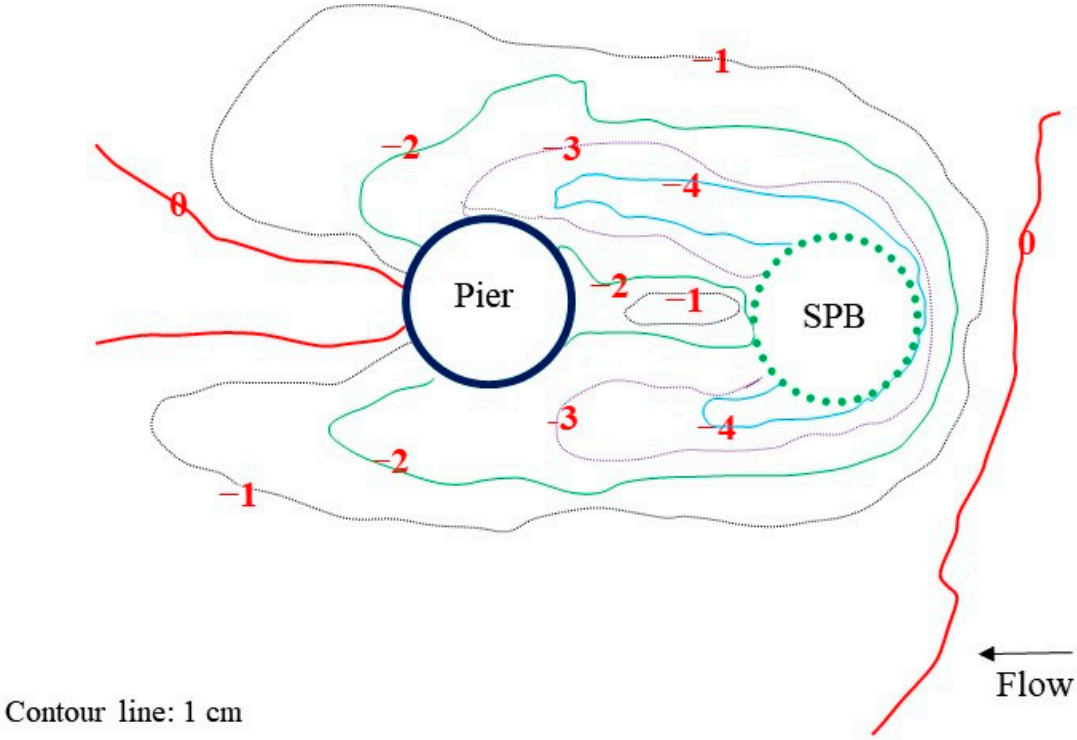


Figure 7. Topography of pier scour with the SPB protection in d = 4 mm, e = 0.5, and L/b = 1.

The purpose of these experiments was to investigate the protective effect of the SBP. This study focused on six geometric parameters regarding the SBP. From the experimental results with and without the SBP, the protective effect can be estimated according to the difference of local scour depth. In each test, the effect of viscous and the influence of ripple-forming bed on the observed depth of local scour cannot be ignored ($d_{50} < 0.7$ mm), and the effect of sidewall was also apparent ($B/b < 10$) [5,22]. These impacts could be offset by comparing the experiments; however, the experimental results were inadequate for a real-world scenario.

4. Result and Discussions

4.1. The Influence of Porosity of SPB on Pier Scour Reduction

Each experiment in this section was performed under fixed flow conditions, $L/b = 1$ and $B_l/H = 1$. Figure 8a shows scour depth around the pier in the cases of PP, OR, A1, A2, and A3. Figure 8b shows scour depth around the pier in the cases of PP, OR, A4, A5, and A6. Figure 8c shows scour depth around the pier in the cases of PP, OR, A7, A8, and A9. In Figure 8, the parameter d_l is the level of sand compared to the initial bed around the pier. If scouring occurs, the value would be negative—positive if deposition occurs.

In the case of PP (w/o protection), the maximum scour depth was located at the front of the pier (phase angle $\phi = 0$). This type of scouring was developed by the occurrence of the down-flow, horseshoe vortex, and wake vortex when the velocity was higher [10]. In the case of OR ($e = 0$), the scouring formation around the pier was similar to the case of PP, but the depth of pier scouring became smaller. That is to say, when the flow passed through a basket without holes ($e = 0$), it caused a sheltering effect to reduce the velocity of approach flow, but the velocity was still large enough to develop the down-flow and horseshoe vortexes around the pier.

As the SPB was set in front of the pier, the maximum scour pier phase angle of $\phi = 90$ or 270 degrees of the pier, which were located at the sides of the pier. The SPB not only produced a sheltering effect to weaken the approach flow but also limited the development of the down-flow in front of the pier. At the same time, the flow velocity near the pier was so small that the horseshoe vortex was not able to fully develop. Hence, the maximum depth of pier scouring shifted to a location nearby the pier side after the SPB was installed. According to the experiments of group A, the reduction in pier scour performed differently due to the influence of SPB porosity. In the case of $d = 3$ mm, the shape and depth of scour were approximately the same between $e = 0.4$ and $e = 0.5$. For other d values (4 mm and 5 mm), the depth of scour decreased as e increased, while the scour formation remained similar. Especially, in the cases of $e = 0.5$ and $d = 4$, 5 mm, nearly no scouring occurred at the front of the pier and deposition even took place at the back of the pier. The maximum pier scour depths (d_s) versus the various porosity (e) of the basket are shown in Figure 9 for $d = 0$, 3, 4, and 5 mm. The scour depth would become generally smaller as the porosity was greater.

The relationship between P and e is illustrated in Figure 9. In Figure 9, P increased as e increased when e was between 0 and 0.5. P was 18.9% when $e = 0$; however, when $e = 0.2$, the value increased quickly to almost 40%. The optimum protection took place under the condition $e = 0.5$ and $d = 4$ mm, in which P reached 75.53%. This demonstrated that the application of the SPB was a superior method for bridge protection against scouring.

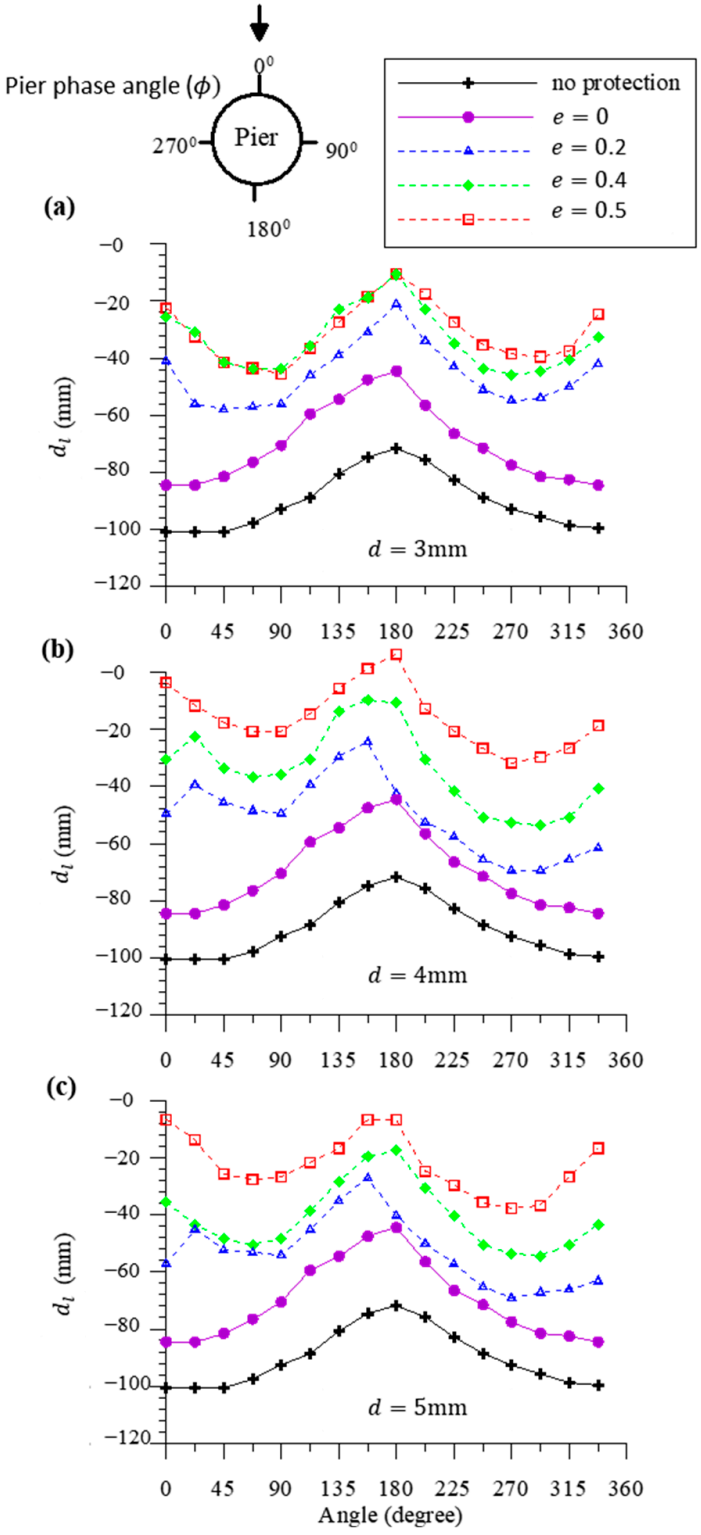


Figure 8. Variation of the sand level around the pier for different basket porosities (*e*): (**a**) In cases of PP, OR, A1, A2, and A3; (**b**) In cases of PP, OR, A4, A5, and A6; (**c**) In cases of PP, OR, A7, A8, and A9.

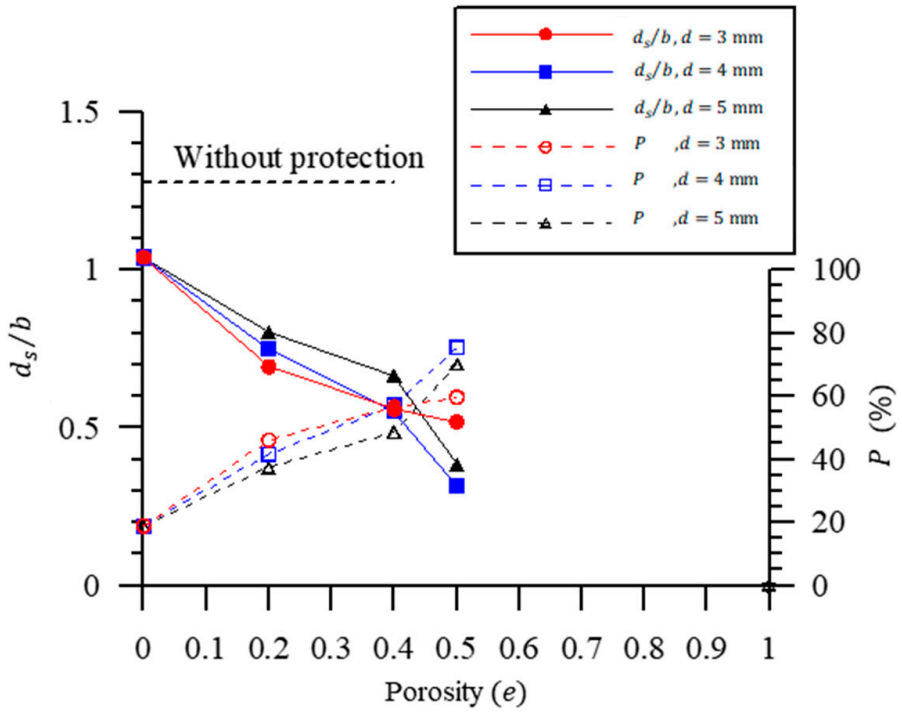


Figure 9. Pier maximum scour depth vs. porosity.

4.2. The Influence of Hole Size of SPB on Pier Scour Reduction

This section discusses the corresponding scouring to various basket hole sizes. According to the cases of group A in Table 2, the protection against bridge scour was stronger as the hole became smaller except for e = 0.5. From the laboratory tests, it was postulated that at the same porosity, SPB at d = 3 mm had a greater number of holes than d = 5 mm, therefore, the number of holes on the SPB surface was a possible factor in the weakening of the approach flow through the porous media. However, this view did not yield consistent results in the case of e = 0.5. The results showed that the protection was improved as the hole was larger when e was smaller than 0.5. For the case e = 0.5, the maximum protective effect took place at d = 4 mm. Importantly, from these experiments, the influence of the hole size of the SPB still remains unclear. Hence, a further study was suggested in which the protective effect should be considered together with the number of holes and hole size.

4.3. The Influence of Distance between Basket and Bridge Pier on Pier Scour Reduction

According to the previous discussion, the best protection conditions—porosity e = 0.5 and hole size d = 4 mm—were selected for further examination. The cases of group B, in Table 2, were used to discuss how the distance of the SPB from the pier would affect the pier scour. Dimensionless values of L/b versus the maximum scour depth ahead of the pier (d_s/b) and the protective effect P were plotted in Figure 10a. This indicated that the maximum scour depth in front of the pier reached its minimum at L/b = 1, which was the best location for pier protection. At this distance, the SPB was able to effectively protect the pier against scouring due to the fact that the flow behind the SPB weakened the down-flow and horseshoe vortex of the pier. Installing the SPB directly in front of the pier did not yield the best results; the SPB must be placed at a certain distance to optimize the result. The maximum scour depth increased as the SPB was moved further away from the pier beyond the point L/b = 1, as seen in Figure 10a. The best pier protection occurred under the condition of L/b = 0.5~2, in which P was over 60%. Contrarily, if the SPB was set directly in front of the pier, P decreased to 49%. When L/b was over 2, P gradually reduced as L/b increased. Even if L/b reached 7, P remained as a high percentage (35%). From the results of scour around the pier (Figure 10b), the maximum scour depth developed at the side of the pier for L/b < 3.5 and developed at the front for all other cases.

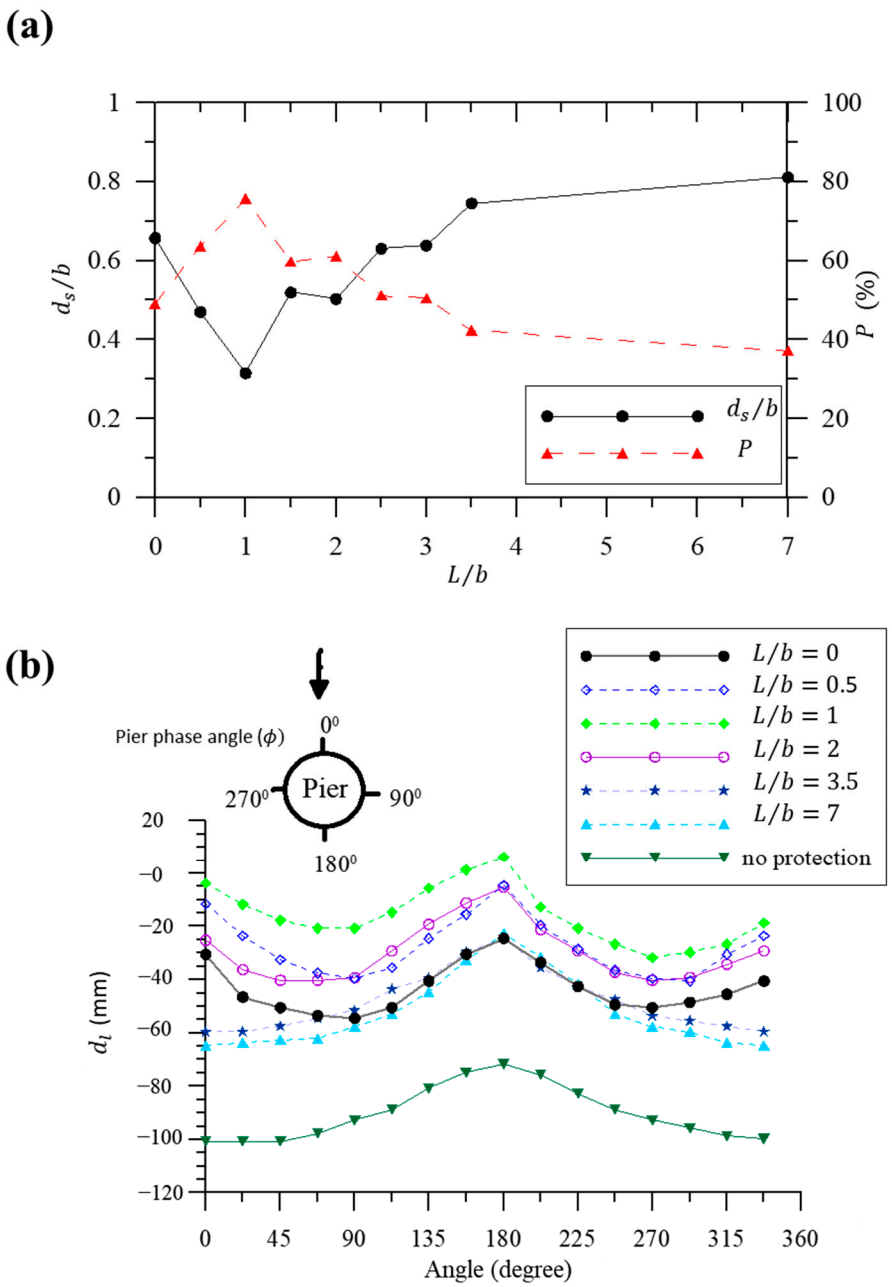


Figure 10. (**a**) Maximum scour depths of pier vs. distances between the SPB and pier; (**b**) variation of sand bed level around pier for different distances between the pier and the SPB.

4.4. The Influence of Height of SPB on Pier Scour Reduction

The flow can pass through the top of the basket without any obstructions when the basket is completely inundated by water, as shown in Figure 3. At this moment, the upper layer flow will directly impede the bridge pier without interference from SPB. According to the cases of group C, in Table 2, the influence of high SPB on pier scour reduction is discussed in this section. Figure 11a shows that the protective effect gradually increased as the height increased in the cases where the SPB was completely inundated by the flow. In this condition, P was able to reach 35.44% when $B_l/H = 0.5$ and reached up to 41.26% when $B_l/H = 1$. However, when the top of the basket protruded from the water surface, the value of P continued to increase up to 75.53% when $B_l/H = 1.3$. This is due to the fact that when $B_l/H = 1$, the rising flow caused by the main horizontal flow, colliding with the SPB, reached the highest point of the SPB, resulting in a flow with fast velocity near the water surface. When $B_l/H = 1.3$, the rising flow could no longer reach the basket; thus, the

results were the same as the other cases when B_l/H = 1.3. From the results of scour around the pier (Figure 11b), the protective effect in front of the pier increased minorly when B_l/H increased from 0 to 1. This is because the approach flow through the immersed SPB was not fully obstructed. When $B_l/H > 1$, the protective effect increased significantly due to the complete obstruction on the approach flow by the SPB.

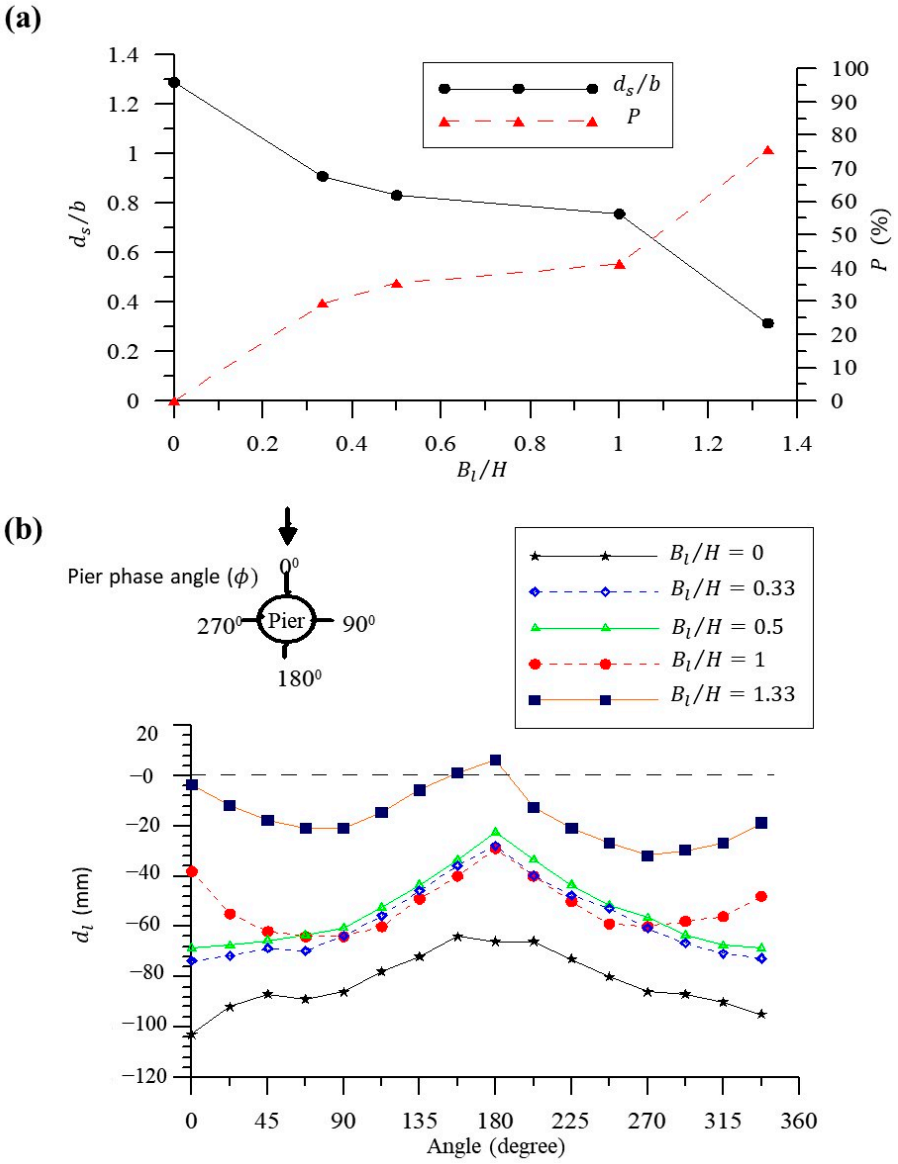


Figure 11. (**a**) Maximum scour depths of pier vs. the different SPB heights; (**b**) variation of the sand bed level around pier for the different SPB heights.

4.5. The Influence of Diameter of SPB on Pier Scour Reduction

To investigate the detailed effects of the basket diameter on the pier protection using the cases of group D in Table 2, the SPB under $\theta = 0°$, L/b = 1, B_l/H = 1.3, and e = 0.5 are discussed herein. The basket diameter had four values, 14, 21, 34, and 80 mm, with shading rates D/b = 17.5%, 26.3%, 42.5%, and 100%. Figure 12 shows that when the shading rate increased, the maximum pier scour depth kept increasing accordingly, demonstrating an obvious linear relationship when D/b > 26.5%. At the smallest shading rate (D/b = 17.5%), although the shading rate was small in this condition, the center velocity of the pier was weakened by the basket. Therefore, a satisfying protective effect, 29.4%, was obtained. This result showed that scouring reduced if the flow at the center of the pier could be weakened.

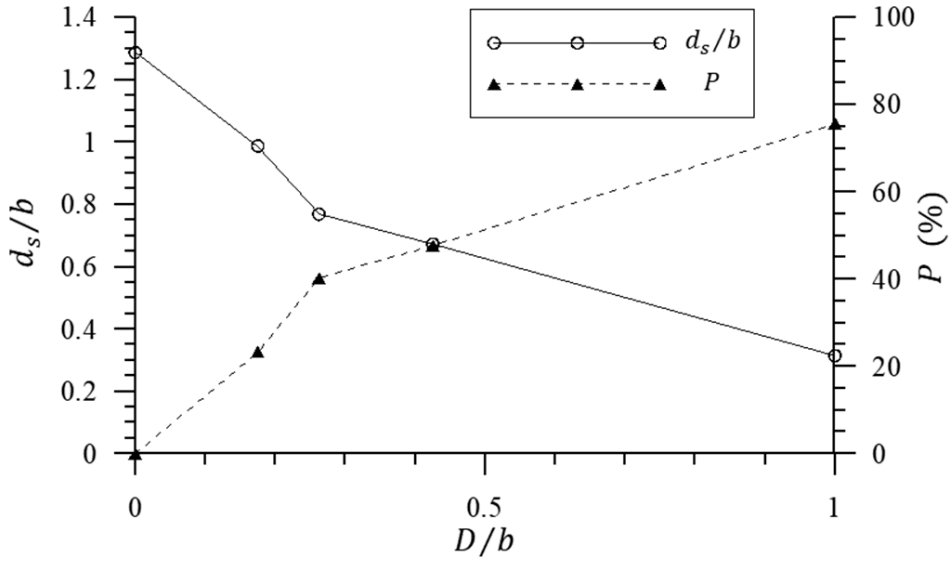


Figure 12. Maximum scour depth around the pier affected by SPB diameter.

4.6. The Influence of Attack Angle (θ) on Pier Scour Reduction

When there is an angle between the direction of the flow and the centerline from the pier to the basket, as shown in Figure 3 (upper part), the partial flow directly attacks the pier. With an increasing attack angle, the pier faces a larger force from the flow which leads to greater scouring. This is to say, the SPB cannot produce a sheltering effect to protect the pier at an increased attack angle. It was found, according to the cases of group E in Table 2, that the protection showed no effect on pier scour if the attack angle was over 30°. The protective effect of P quickly dropped from 75.53% to 12.8% when θ changed from 0 to 30 degrees. The maximum scour depth at $\theta = 45°$ was larger than the pure pier scour depth. This clearly demonstrates that the SPB must be set at $\theta = 0°$.

4.7. Discussions

According to the results from this study, the protective effect of SPB, which is a new type of combined flow-altering countermeasure, can be evaluated. First, the SPB was similar to the sacrificial piles—it provided a kind of sheltering effect to against the approach flow—therefore, the strengths of the down-flow and the horseshoe vortex decreased [5]. This paper also found that the porosity, the diameter, and the attack angle of the SPB determined the performance of the sheltering effect. With conditions $e = 0.5$, $D/d = 1$, and $\theta = 0°$, the pier scour reduction reaches the maximum. Second, as shown in Figure 2, the SPB was also similar to the surface guide panels—the flow velocity of the bed was increased as it approached the SPB, therefore, the local sediment at the SPB was carried downstream and deposited into the scour hole at the pier [5]. The distance between the SPB and the pier (L/b) plays an important role in this effect. As L was too short, this effect could not fully perform. After the sediment was carried from the bed near the SPB, it could not be transported too far to reach the local hole. This paper suggests that the value of L must be between $0.5b$ and $3b$. Finally, this paper found that the strength of surface flow near the SPB influences the performance of down-flow at the head of the pier. When the SPB was immersed, it did not completely obstruct the surface flow through the SPB, therefore, the weakening of the down-flow at the head of the pier was obvious. In other words, as $B_l/H > 1$, the down-flow at the head of the pier can be decreased so that the depth of pier scour is reduced. This paper implied that this new type of combined flow-altering countermeasure could be a potential option to protect the local scour nearby the bridge pier.

This subsection highlights some limitations in this study. First, this study investigated the geometric feature of SPB on the protective effect of pier scour, for example, SPB porosity, hole size, height, attack angle, and distance between SPB and the pier. However, many researchers have pointed out that hydraulic features and sediment features are also important effects on the variation of pier scour; for instance, the effect of flow intensity, Froude number, non-uniform particle size distribution material, and median distribution particle size [10,12–15]. The performance of the protective effect of SPB in the field application was not confirmed due to these aforementioned limitations. Second, the experimental design in clear water did not control for the equilibrium pier scour to reach the maximum value. According to the pier channel width and diameter ratio, the side-wall effect exists to influence the development of pier scour nearby the channel's wall [5]. The chosen sediment ($d_{50} < 0.7$ mm) was too fine to avoid the viscous effect and the influence of the ripple-forming bed [5,22]. If the aforementioned effects cannot be avoided in the pier scour test, the observed depth of the pier scour might lead to erroneous results. Third, this study only recorded the bed level variation in the experiment. However, the velocity field measurement plays an important role in justifying the turbulent dynamics therein produced and, ultimately, on the erosion levels. Recording the velocity field, the influence of SPB on the development of down-flow, horseshoe vortex, and wake vortex would be useful for further studies.

5. Conclusions

In this paper, the use of the single porous basket (SPB) was examined in detail, and the results showed that SPB indeed produced a favorable sheltering effect by weakening the downstream flow ahead of the pier and the horseshoe vortex around it. Both flow-altering effects showed significant improvements to pier protection. This study showed that, from the clear water experiment, the performance of the SPB was affected by several setup factors for the pier scour. The best setup conditions were found to be $e = 0.5$, $\theta = 0°$, $L/b = 1$, $D/d = 1$, and $B_l/H = 1.3$. Under these conditions, the best scour reduction ratio was up to 75.53%. If a protective effect over 50% was attempted in the tests, the value of L must be between $0.5b$ and $3b$. In shallow water conditions, the basket must be set over the water surface for an optimum shading effect. Most importantly, the SPB must be aligned with the flow direction, so that $\theta = 0°$.

This paper presents preliminary research on the investigation of a new type of combined flow-altering countermeasure. From a series of experiments, the protective effect of SPB can be estimated according to its geometric features. The performance of SPB in field applications has not sufficiently been investigated. In future studies, the influence of hydraulic and sediment features will be considered. In order to enhance the performance of the experiment, the experimental design should reduce the side-wall effects, sediment size, flow shallowness, and time, and the recorded data should also include the velocity field.

Author Contributions: Conceptualization, C.-K.H. and C.-W.L.; methodology, C.-K.H. and C.-W.L.; formal analysis, C.-K.H., C.-W.L. and W.-L.L.; wrote the manuscript, C.-W.L. and W.-L.L. All authors contributed to improving the paper. All authors have read and agreed to the published version of the manuscript.

Funding: This research received no external funding.

Institutional Review Board Statement: Not applicable.

Informed Consent Statement: Not applicable.

Data Availability Statement: Not applicable.

Conflicts of Interest: The authors declare no conflict of interest.

Notation

The following symbols are used in this paper:

A	total surface area of the basket;
A_0	the total hole area of the basket;
B_d	depth of basket under water;
B_l	length of basket;
b	diameter of pier;
D	diameter of SPB;
d	hole size;
d_{50}	median size of the sediment;
d_l	the level of bed around the pier;
d_s	the max. scour depth of the pier with SPB protection;
d_{sn}	the max. scour depth of the pier without any protection;
e	porosity;
g	specific gravity of sand;
H	average depth of flow;
K_d	particle shape factor;
K_l	basket shape factor;
L	distance between panel and pier;
P	the percentages in maximum scour depth reduction ratio at pier;
V	average velocity;
V_c	mean velocity at threshold of motion of bed material;
θ	skew angle between the approach flow and basket axis;
ϕ	phase angle at pier;
ρ	fluid density;
ν	kinematic viscosity of water;
ρ_s	specific gravity of sand;
σ_g	geometric standard deviation.

References

1. Kao, S.J.; Lee, T.Y.; Milliman, J.D. Calculating highly fluctuated suspended sediment fluxes from mountainous rivers in Taiwan. *Terr. Atmos. Ocean. Sci.* **2005**, *16*, 653. Available online: https://scholarworks.wm.edu/vimsarticles/102/ (accessed on 29 October 2021). [CrossRef]
2. Khan, K.A.; Muzzammil, M.; Alam, J. Bridge Pier Scour: A review of mechanism, causes and geotechnical aspects. *Proc. Adv. Geotech. Eng.* **2016**, 8–9. Available online: https://www.reserachgate.net/publication/312499136_Bridge_Pier_Scour_A_review_of_mechanism_causes_and_geotechnical_aspects (accessed on 29 October 2021).
3. Melville, B.W.; Hadfield, A.C. Use of sacrificial piles as pier scour countermeasures. *J. Hydraul. Eng.* **1999**, *125*, 1221–1224. [CrossRef]
4. Chiew, Y.M. Scour protection at bridge piers. *J. Hydraul. Eng.* **1992**, *118*, 1260–1269. [CrossRef]
5. Tafarojnoruz, A.; Gaudio, R.; Dey, S. Flow-altering countermeasures against scour at bridge piers: A review. *J. Hydraul. Res.* **2010**, *48*, 441–452. [CrossRef]
6. Lauchlan, C.S. Countermeasures for Pier Scour. Ph.D. Thesis, The University of Auckland, Auckland, New Zealand, 1999. Available online: https://trid.trb.org/view/855383 (accessed on 29 October 2021).
7. Huang, C.K.; Tang, C.J.; Kuo, T.Y. Use of Surface Guide Panels as Pier Scour Countermeasures. *Int. J. Sediment Res.* **2005**, *20*, 117–128.
8. Khaple, S.; Hanmaiahgari, P.R.; Gaudio, R.; Dey, S. Splitter plate as a flow-altering pier scour countermeasure. *Acta Geophys.* **2017**, *65*, 957–975. [CrossRef]
9. Gaudio, R.; Tafarojnoruz, A.; Calomino, F. Combined flow-altering countermeasures against bridge pier scour. *J. Hydraul. Res.* **2012**, *50*, 35–43. [CrossRef]
10. Melville, B.W.; Coleman, S.E. *Bridge Scour*; Water Resources Publication: Littleton, CO, USA, 2000.
11. Ettema, R.; Mostafa, E.A.; Melville, B.W.; Yassin, A.A. Local scour at skewed piers. *J. Hydraul. Eng.* **1998**, *124*, 756–759. [CrossRef]
12. Bozkus, Z.; Yildiz, O. Effects of inclination of bridge piers on scouring depth. *J. Hydraul. Eng.* **2004**, *130*, 827–832. [CrossRef]
13. Ettema, R. *Scour at Bridge Piers*; Auckland University: Auckland, New Zealand, 1980. Available online: https://trid.trb.org/view/171850 (accessed on 29 October 2021).
14. Chiew, Y.M. *Local Scour at Bridge Piers*; Auckland University: Auckland, New Zealand, 1984. Available online: http://trid.trb.org/view/277693 (accessed on 29 October 2020).

15. Baker, R.E. *Local Scour at Bridge Piers in Non Uniform Sediment*; Auckland University: Auckland, New Zealand, 1986. Available online: https://trid.trb.org/view/1196837 (accessed on 29 October 2020).
16. Chee, R.K.W. *Live-Bed Scour at Bridge Piers*; Auckland University: Auckland, New Zealand, 1982. Available online: http://trid.trb.org/view/271201 (accessed on 29 October 2020).
17. Raudkivi, A.J. Functional trends of scour at bridge piers. *J. Hydraul. Eng.* **1986**, *112*, 1–13. [CrossRef]
18. Melville, B.W. The physics of local scour at bridge piers. In Proceedings of the 4th International Conference on Scour and Erosion (ICSE-4), Tokyo, Japan, 5–7 November 2008; pp. 28–40. Available online: https://hdl.handle.net/20.500.11970/100095 (accessed on 29 October 2021).
19. Raudkivi, A.J.; Ettema, R. Effect of sediment gradation on clear water scour. *J. Hydraul. Div.* **1977**, *103*, 1209–1213. [CrossRef]
20. Melville, B.W.; Sutherland, A.J. Design method for local scour at bridge piers. *J. Hydraul. Eng.* **1988**, *114*, 1210–1226. [CrossRef]
21. Melville, B.W.; Chiew, Y.M. Time scale for local scour at bridge piers. *J. Hydraul. Eng.* **1999**, *125*, 59–65. [CrossRef]
22. Oliveto, G.; Hager, W.H. Further results to time-dependent local scour at bridge elements. *J. Hydraul. Eng.* **2005**, *131*, 97–105. [CrossRef]